

PACS numbers: 42.55.Lt;42.60.Lh
DOI: 10.1070/QE2011v041n12ABEH014713

Lasing from the domain of collision of ionisation waves produced due to electric field concentration at electrodes with a small radius of curvature

V.F. Tarasenko, A.E. Tel'minov, A.G. Burachenko, D.V. Rybka,
E.Kh. Baksht, M.I. Lomaev, A.N. Panchenko, P.O. Vil'tovskii

Abstract. **The characteristics of UV lasing in nitrogen and of diffusive discharge produced without an additional ionisation source were experimentally investigated in a nonuniform electric field formed by electrodes with different profiles. High-voltage nanosecond pulses were applied to the blade- and cylinder-shaped electrodes. It was determined that the gap breakdown at elevated pressure was caused by diffusive jets which propagate from the electrodes with a small radius of curvature. The electric field increased in the intersection of counter-propagating jets, with the effect that the threshold of lasing in the $C\,^3\Pi_u - B\,^3\Pi_g$ (λ = 337.1 nm) molecular nitrogen band was attained for low average electric fields (below 60 V cm^{-1} Torr^{-1}) and at pressures of 760 Torr and above. With lowering the pressure from 760 to 20 Torr, the voltage of gap breakdown in the nonuniform electric field was observed to increase for a voltage pulse rise time of ~300 ps and to decrease for a pulse rise time of ~2 ns.**

Keywords: *diffusive discharge, nonuniform electric field, elevated pressure, transverse discharge pumping, UV lasing in nitrogen.*

1. Introduction

For the pumping of the majority of pulsed high-pressure gas lasers, use is made of longitudinal or transverse glow discharges (normal and anomalous) [1–4]. For several lasers in which the excitation of the upper laser level requires high electron temperatures, advantage is taken of the breakdown stage, wherein the voltage across the discharge gap lowers several-fold in a fraction of a nanosecond or in a few nanoseconds [2]. Under these conditions, the high intensities of the electric field in the discharge gap are achieved by way of application of voltage pulses with a steep edge. A volume (diffusive) discharge at an elevated pressure is formed due to the preionisation of the gap by an additional source, which ensures the overlapping of avalanche heads [5]. The use of profiled electrodes permits lowering the initial electron density and broadening the range of conditions for the formation of a pulsed diffusive discharge [1–3]. Special mention should be made of lasers which employ a volume discharge at a pressure of 1 atm and above, which is triggered or stabilised by an electron beam [2, 3]. The flux of high-energy electrons formed in vacuum diodes efficiently produces the preionisation of the gap, and the working pressure of a laser mixture may be as high as several tens of atmospheres.

The application of electrodes with a small radius of curvature makes it possible to realise the regime of diffusive discharge formation, whereby the runaway electrons generated in the same discharge gap bring about the preionisation of the gap. Under these conditions, the gap breakdown takes place in the formation of an ionisation wave, which propagates from the electrode with a small radius of curvature (see Ref. [6] and references therein). This regime of forming a diffusive discharge at elevated pressures was supposedly realised in the study of avalanches and streamers early in the past century. Its realisation necessitates the use of voltage pulses with a nanosecond rise time (see, for instance, Ref. [7]). However, neither the runaway electrons nor the X-ray radiation from the discharge domain were recorded in the first papers. The formation of a diffusive discharge in the recording of X-ray radiation from helium and air atmospheric-pressure discharge gaps was first reported in Refs [8] and [9], respectively. The conditions for the generation of a supershort avalanche electron beam (SAEB) with the highest amplitudes in the air at atmospheric pressure and in other gases were described in detail in reviews [10, 11]. It is noteworthy that the use of X-ray radiation generated due to runaway electrons in an additional gap for the preionisation in wide-aperture lasers was reported in Refs [12, 13]. We also note that the threshold of lasing in the $C\,^3\Pi_u - B\,^3\Pi_g$ molecular nitrogen band is not reached when elevated-pressure nitrogen is excited by an electron beam alone due to the excitation of the lower laser level by plasma electrons [14].

Lasing in the formation of a discharge due to runaway electrons generated in the same gap at a pressure above 1 atm was reported in Refs [15, 16]. Laser radiation was generated on IR transitions in xenon [15] and at a wavelength λ = 337.1 nm in nitrogen [16]. The lasing in an $N_2:SF_6 = 10:1$ mixture was recorded at a high pressure (up to 2.5 atm). In Refs [15, 16] the pumping was effected by a transverse discharge and the ionisation waves propagated perpendicular to the resonator axis. Studied in several papers (see, for instance, Ref. [17]) was the breakdown in long tubes due to an ionisation wave, but to obtain lasing in nitrogen use was made of a longitudinal discharge at relatively low pressures. In recent work [18], lasing in nitrogen was obtained from the domain of collision of diffusive jets (ionisation waves), which propagated from opposite electrodes. However, this pumping regime was not investigated in detail.

V.F. Tarasenko, A.E. Tel'minov, A.G. Burachenko, D.V. Rybka, E.Kh. Baksht, M.I. Lomaev, A.N. Panchenko, P.O. Vil'tovskii Institute of High Current Electronics, Siberian Branch, Russian Academy of Sciences, Akademicheskii prosp. 2/3, 634055 Tomsk, Russia;
e-mail: VFT@loi.hcei.tsc.ru

Received 1 September 2011
Kvantovaya Elektronika **41** (12) 1098–1103 (2011)
Translated by E.N. Ragozin

The objective of our work is to study the conditions for UV lasing in nitrogen pumped by a transverse discharge at elevated pressure for a gap breakdown by ionisation waves. In this work we continue the investigations undertaken in Ref. [18].

To reveal the location of discharge gap domains of enhanced electric field, use was made of the laser radiation in the second positive system of nitrogen with $\lambda = 337.1$ nm. Effective lasing at this wavelength is possible only for large values of the E/p parameter, where E is the electric field intensity and p is the nitrogen pressure [19]. High E/p values (above 100 V cm^{-1} Torr^{-1}) are achieved at elevated pressures (the right branch of the Paschen curve) only for a rise time of the voltage pulse (normally tens of nanoseconds). Under these conditions, the amplitude of the voltage pulse is highest and then, in the gap breakdown, E/p rapidly (in a fraction of a nanosecond or in a few nanoseconds) decreases because of the avalanche multiplication of electrons. In the quasi-stationary stage of the volume (diffusive) discharge in pure nitrogen, which sets in after the rapid droop of the voltage across the gap, the E/p parameter value is relatively small ($\sim$40 V cm^{-1} $\times$ Torr^{-1}) and the lasing on the $C\,^3\Pi_u - B^3\Pi_g$ transition terminates. When the gap breakdown occurs at low E/p values (lower than 80 V cm^{-1} Torr^{-1}), the threshold of lasing in nitrogen is ordinarily not reached even at the stage of rapid voltage decrease. In Ref. [20], an electric field enhancement in propagation of ionisation wave through the gap was recorded using the Stark effect for low xenon pressures and a submicrosecond time resolution. Experiments to directly measure the electric fields were carried out employing two lasers with different wavelengths and an ICCD camera in Ref. [20].

2. Experimental facility and measurement technique

We investigated lasing under pumping by a RADAN-220 nanosecond pulse generator (facility 1) with a 20-Ω wave impedance of the high-voltage line. The amplitude of the voltage pulse on a high-resistance load was equal to $\sim$220 kV. The half-amplitude duration of the voltage pulse on a matched load was equal to about 2 ns and the rise time of the voltage pulse in the transmission line was equal to 0.5 ns. On connecting up the discharge chamber, the rise time of the voltage pulse lengthened to 2 ns, its half-amplitude duration also became longer. The duration of the discharge current pulse depended of the pressure and sort of gas; at low pressures, it could amount to several hundred nanoseconds in an oscillation regime. The discharge chamber design is schematically shown in Fig. 1. In these experiments we employed a gap with a cathode–anode separation of 12 or 20 mm. Both electrodes were made in the form of blades with rounded edges or one electrode had the shape of a blade and the other was cylindrical with a radius of curvature of $\sim$6 mm. The length of the discharge region was equal to 20 cm, which permitted obtaining UV lasing in nitrogen as well as lasing in other gases. In the case when one electrode was cylindrical and the other was blade-shaped, our experiments were carried out for different polarities of the voltage pulse. The chamber was evacuated with a diffusion pump and could be filled with different gases. Resonator mirrors were mounted on the end walls of the discharge chamber. An additional window intended for photographing the discharge was located on the side wall of the chamber.

The amplitude-time characteristics of the UV laser radiation were recorded with an FEK-22SPU photodiode. The gap region which emanated the laser radiation was determined

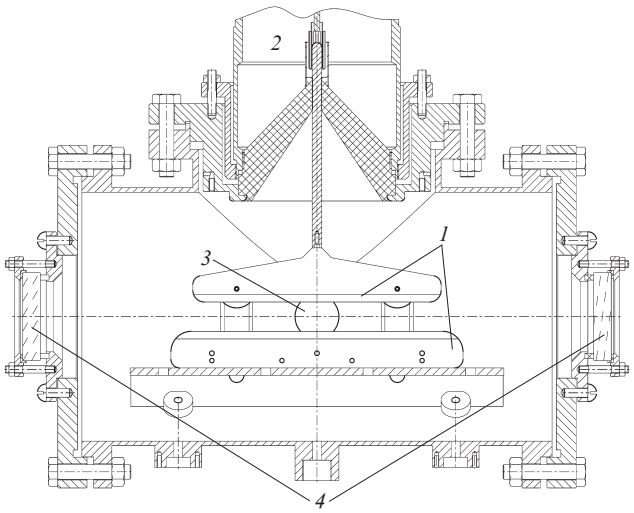

Figure 1. Structure of discharge chamber of facility 1: (*1*) electrodes; (*2*) output part of RADAN-220 generator; (*3*) side window; (*4*) resonator mirrors.

from the luminescence of the screen mounted on the output mirror. The discharge and luminescent screen glows were photographed with a Sony A100 digital camera. The spectrum of laser radiation was recorded using a StellarNet EPP2000-C25 spectrometer with a resolution of 0.75 nm. To operate the photodiode and the spectrometer in a linear regime, the radiation was attenuated with a series of metal meshes at input. Also recorded in experiments were the discharge current and the voltage across the laser electrodes with the use of an ohmic voltage divider and a shunt. A TDS-3054B (0.5 GHz, 5 samplings per 1 ns) oscilloscope was employed to record electric signals.

Furthermore, the discharge characteristics and the runaway electron current (an ultrashort avalanche electron beam) were investigated on the second facility with a small volume under excitation, to which voltage pulses from a SLEP-150 generator were applied [10]. The SLEP-150 generator (without a transmission line) produced voltage pulses with an amplitude of 140–170 kV on a high-resistance load. In the transmission line the amplitude of the incident voltage wave was equal to 130–150 kV. In this case, the pulse rise time was equal to $\sim$300 ps at a 0.1–0.9 level and the half-amplitude duration of the voltage pulse was equal to $\sim$1 ns in the case of a matched load. The employment of transmission line in the SLEP-150 generator permitted measuring the incident and reflected voltage waves and reconstructing the voltage across the gap during the generation of the runaway electron beam [10, 11]. The separation of the planar anode from the cathode was equal to 12 mm. The function of the cathode was fulfilled by a tube $\sim$6 mm in diameter made of 100-μm thick steel foil. On facility 2 it was possible to measure the discharge current, the SAEB current and the voltage using a DPO70604 oscilloscope (6 GHz, 25 samplings per 1 ns) with a time resolution as high as 100 ps. Because the active length was short ($\sim$10 mm), the lasing threshold was not reached on this facility.

3. Experimental results and their discussion

The characteristics of discharge and radiation were investigated in nitrogen, neon, and a neon–hydrogen mixture. The pressure in the gap was varied from 1 to 3000 Torr. A diffu-

sive discharge was formed in all gases in a broad pressure range; the discharge consisted of jets, which overlapped at low pressures. Lasing was obtain at $\lambda = 337.1$ nm in nitrogen and in the air and at $\lambda = 585.3$ nm in the mixture of neon with hydrogen. Due to an increase in active length, the output power obtained in pure nitrogen was higher than the output power obtained with the same generator in the experiment described in Ref. [16]. In the mixture of neon with hydrogen, owing to the oscillation regime of discharge, which is not optimal for a Penning neon plasma laser [2] operating in the afterglow regime, the output power was low and was therefore not investigated in detail.

Facility 2 was employed to record the pulses of discharge current and voltage as well as of the runaway electron beam current with subnanosecond time resolution. Figure 2 shows the oscilloscope traces of discharge current pulses, the SAEB current, and the voltage across the gap for an air pressure of 760 Torr. The discharge current was measured only in the air, because the application of a shunt with a high time resolution did not permit evacuating the discharge chamber. The SAEB oscilloscope traces were recorded behind the anode made of 15-μm-thick aluminium foil. All oscilloscope traces were synchronised in time. The SLEP generator results in the formation of a diffusive discharge at elevated pressures and the decrease in the voltage across the gap. The magnitude of the gap breakdown voltage depends on the rise time of the voltage pulse. The magnitude of the voltage in the quasi-stationary stage of discharge depends on the pressure and sort of gas, all other conditions being the same. As is well known [2], in pure nitrogen the voltage in the quasi-stationary stage is equal to ~40 В cm^{-1} $Torr^{-1}$. Because of the distortions introduced by reflected pulses, shown in Fig. 2 is only the initial period of this stage. Like in the formation of a pulsed space charge with preionisation from an additional source, in the oscilloscope traces of the voltage pulse it is possible to single out three main stages: the pulse edge, the stage of rapid voltage decrease, and the quasi-stationary stage, whose duration corresponds under our conditions to about the duration of the generator pulse. The two first stages of the voltage pulse are depicted in Fig. 2 for a subnanosecond time resolution of the recording system. The oscilloscope traces of the quasi-stationary stage of discharge in nitrogen may be found in many papers (see, for instance, Refs [2, 19]). As shown in these works (see also references therein), efficient excitation of the upper laser level of the $C\,^3\Pi_u - B^3\Pi_g$ transition in the UV lasing in nitrogen takes place only at the stage of rapid decrease in the voltage across the gap.

Lasing and the discharge characteristics were investigated on facility 1. When two blade electrodes were used, diffusive jets originated from both electrodes and overlapped approximately at a distance of 1/3 from the anode. In the case of one blade electrode and one cylindrical electrode, diffusive jets originated from the electrode with a small radius of curvature and propagated towards the cylindrical electrode to reach it in 1–3 ns. The diameter of the diffusive jets became smaller with increasing the nitrogen pressure in the discharge chamber. The gap breakdown voltage depended on the sort and pressure of gas as well as on the rise time of the voltage pulse. As the nitrogen pressure was increased from 150 Torr to 2 atm, the voltage across the 2-cm long discharge gap increased approximately from 65 to 170 kV. The dependence of the gap breakdown voltage on the pressure for a 1.2-cm gap is plotted in Fig. 3a. Shortening the interelectrode gap, as would be expected, resulted in a lowering of the breakdown voltage. It was found that the pressure dependences of the gap breakdown voltage obtained on facilities 1 and 2 were significantly different. For a subnanosecond duration of the pulse front, the breakdown voltage increased with decreasing pressure on facility 2 (Fig. 3b); for a nanosecond front duration the breakdown voltage lowered on facility 2 (Fig. 3a).

With lengthening the rise time of the voltage pulse, the diffusive jets became smaller in diameter and spark leaders began to grow from the electrodes; under these conditions, the spark leaders amounted to several millimetres in length. The discharge uniformity in the air was lower than in nitrogen. In this case, under similar experimental conditions the diffusive jets in the air were smaller in diameter and the spark leaders began growing at lower pressures. In neon and hydrogen as well as in their mixtures, the discharge uniformity was higher in comparison with discharges in the air and nitrogen.

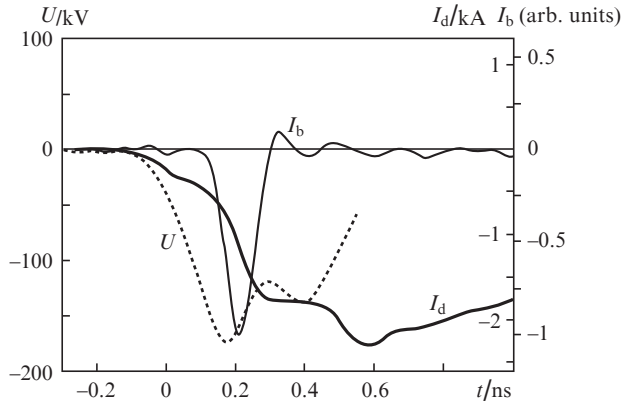

Figure 2. Oscilloscope traces of the voltage across the discharge gap (U), the discharge current (I_d), and the runaway electron beam current (I_b) (facility 2).

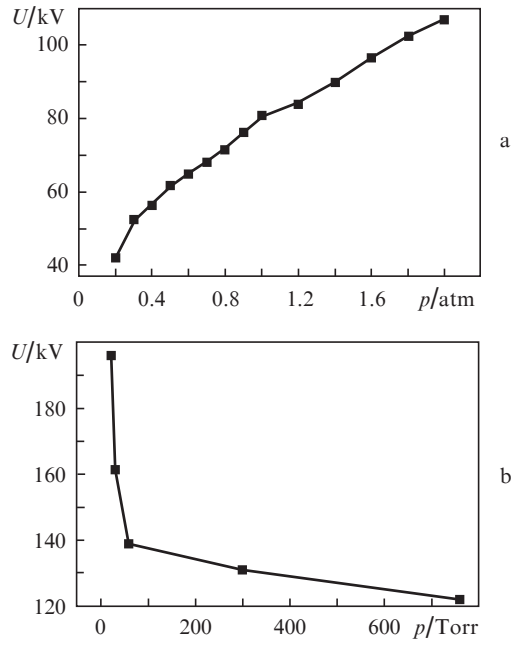

Figure 3. Dependences of the amplitude of the voltage across the discharge gap on the gas pressure, which were obtained on facility 1 (a) and facility 2 (b). The interelectrode distance is equal to 12 mm.

Figure 4 serves to illustrate the main result of our work. The highest values of the E/p parameter were achieved for low nitrogen pressures on facility 1, despite the lowering of the gap breakdown voltage. Specifically, for a nitrogen pressure of 150 Torr the average value of the E/p parameter was equal to $\sim$210 V cm^{-1} Torr^{-1}. To determine E/p from oscilloscope traces, the maximum value of the voltage across the gap was divided by the gap width and the gas pressure. As is clear from Fig. 4a, the highest power density of laser radiation at a low density was recorded from near-electrode regions, where the electric field and the discharge current density are enhanced due to the blade-like shape of the electrodes. In this case, lasing is also observed from the domain adjacent to the side surface of the anode. In the central part of the gap (closer to the anode), the power density of laser radiation becomes lower, which may be attributed both to the lowering of the E/p parameter in the central part of the gap and to its increase above the optimal value. With increasing nitrogen pressure, the 'pattern' of laser radiation is substantially changed (Fig. 4b). In the middle of the gap (closer to the anode), for an invariable resonator alignment there appears the third lasing spot. For a nitrogen pressure of 2 atm, the average value of the E/p parameter amounts to only 55 V cm^{-1} Torr^{-1} for the maximum voltage across the gap. The threshold of lasing in nitrogen should not be reached for this value of the E/p parameter. In the vicinity of blade electrodes, the electric field is higher than the average one and lasing does take place, as is evident from Fig. 4b. For low average values of the E/p parameter, the lasing threshold in these regions is attained due to electric field enhancement near both electrodes. Furthermore, near the electrodes the discharge current densities are maximal, which increases the intensity of pumping and favours the attainment of the lasing threshold. The emergence of the third laser beam in the discharge gap is attributable only to the enhancement of electric field in this region. To obtain efficient lasing requires, as noted above, that E/p should be no less than 100 V cm^{-1} Torr^{-1}. Consequently, in the development of gap breakdown there is a phase with a substantial enhancement of the electric field in the gap.

As follows from our experiment (Fig. 4), the region of enhanced electric field, which is detected by the emergence of UV lasing in nitrogen, makes its appearance in the interspace between the fronts of ionisation waves (diffusive jets); in the motion of the waves towards each other, the greatest enhancement of the electric field at elevated nitrogen pressure should take place in that part of the gap where these waves meet. One can see from the distribution of intensity of laser radiation and the gap glow intensity that lasing takes place in that part of the gap which exhibits a weaker glow (Fig. 4b). Figure 4c is the photograph of discharge taken under the same conditions for a higher camera responsivity. This photograph suggests that the region of lasing is the site of mixing of the diffusive jets, which propagate towards each other from the cathode and the anode. The picture of the 'coalescence' of the diffusive jets varies lengthwise of the electrodes. In particular, in the mixing of three jets directed towards the anode with one jet directed towards the cathode (region 1 in Fig. 4c), the brightness of the emission of the latter exhibits an enhancement, and a higher-brightness spot is seen at the anode. A similar picture is seen in another gap region (region 2), but in this case several cathode-directed jets close to one jet directed towards the anode. Furthermore, one can see the intersection of oppositely directed jets at an angle to their propagation direction. On shortening the interelectrode gap to 12 mm, the character of discharge remains unchanged under variations of the pressure, the dark band spaced from the anode at about one third of the length persists, and the third laser beam emanates from this region at elevated nitrogen pressures. Figure 5 shows the time delay between the moment the discharge current reaches its peak and the onset of lasing as a function of nitrogen pressure. The delay of the onset of lasing shortens with increasing pressure and is hardly changed at pressures of 1–2 atm.

The time characteristics of laser radiation are also testimony to the rise of the electric field in the gap in the propaga-

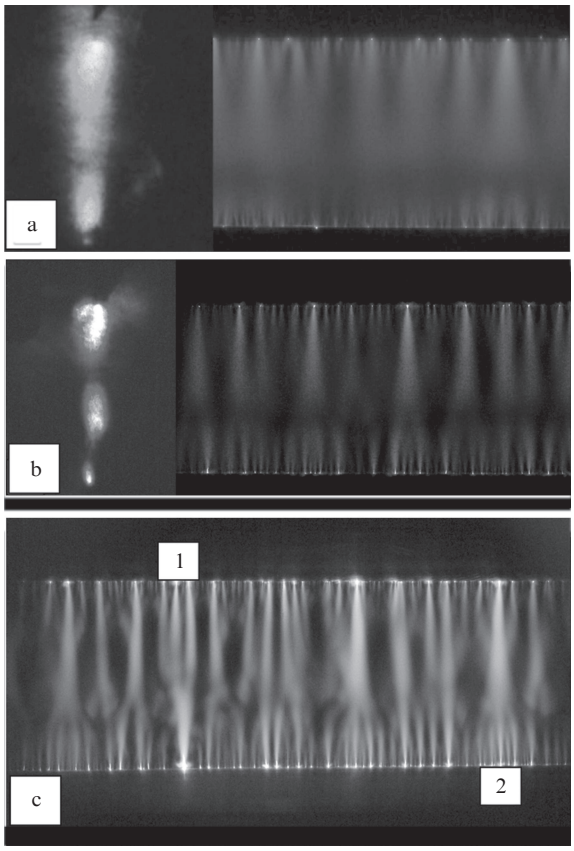

Figure 4. Photographs of discharge glow and lasing (at the left of Figs 4a and 4b) for a nitrogen pressure of 0.2 (a) and 2 atm (b, c) and the highest voltage across the gap of 65 (a) and 170 kV (b, c). The interelectrode gap is equal to 2 cm. Photograph (c) was taken for a higher responsivity of the camera (facility 1).

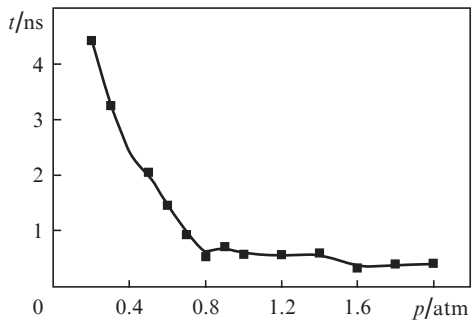

Figure 5. Pressure dependence of the delay between the discharge current peak and the onset of lasing in pure nitrogen for an interelectrode gap of 12 mm (facility 1).

tion of ionisation waves. Figure 6a shows the pulses of lasing from near-electrode regions and the central part of the gap for an interelectrode distance of 12 mm and a nitrogen pressure of 2 atm. Initially the lasing emerges at the cathode and then, with a delay of ~0.2 ns, at the anode. As noted above, the electric field in these domains is maximal prior to the onset of ionisation in the gap. Then, with a delay of ~1 ns, lasing emerges in the central part of the gap [oscilloscope trace (*3*) in Fig. 6a]. When the nitrogen pressure is lowered from 2 to 1 atm, the power of lasing becomes higher (Fig. 6b), while the delay between the peak of discharge current and the onset of lasing in pure nitrogen is hardly changed (Fig. 5). When the pressure becomes lower than 0.8 atm, the lasing regime begins to change (Fig. 6c). The delay of the onset of the laser pulse becomes longer (Fig. 5) and the radiation is more evenly distributed over the entire discharge gap. The highest output power was obtained for a pressure of 0.4 atm in a radiation pulse containing one peak. When the pressure is less than 1 atm, the ionisation wave velocity is higher [17] and the breakdown of the entire gap takes place in a shorter time. The increase in lasing delay with lowering pressure may be attributed to a decrease in the number of molecules in the $C\,^3\Pi_u$ state. As discussed above, with lowering nitrogen pressure on facility 1, the gap breakdown voltage becomes lower.

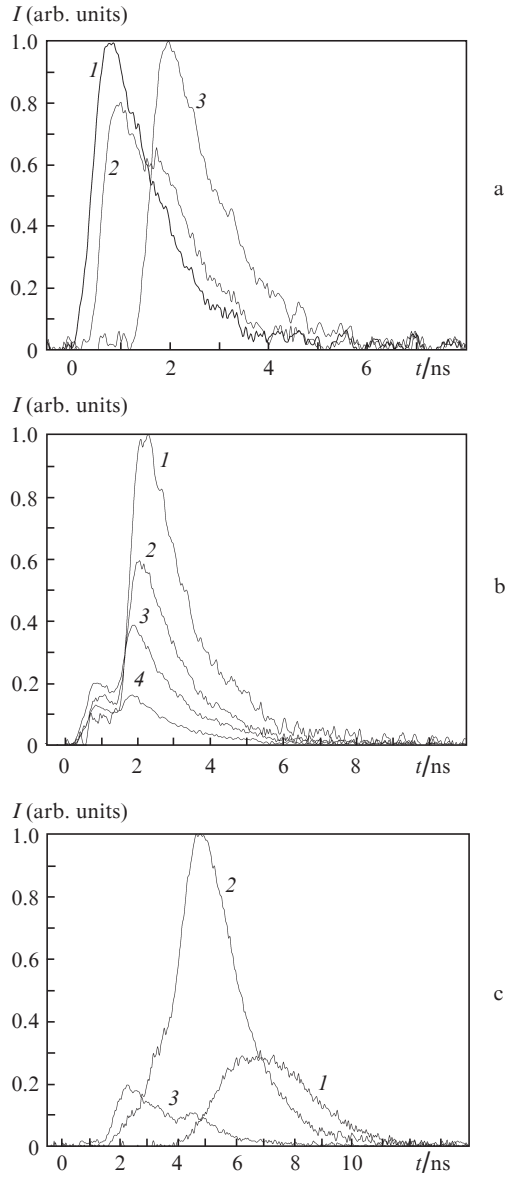

Figure 6. Oscilloscope traces of lasing obtained on facility 1 from different gap regions [(*1*) – near the upper electrode, (*2*) – near the lower electrode, (*3*) – in the central part] for a nitrogen pressure of 2 atm (a), oscilloscope traces of lasing obtained from the entire gap at pressures of 1 (*1*), 1.2 (*2*), 1.6 (*3*), and 2 atm (*4*) (b); oscilloscope traces of lasing from the entire gap at pressures of 0.2 (*1*), 0.4 (*2*), and 0.8 atm (*3*) (c).

Figure 7 displays the patterns of the laser beam on replacing the lower electrode with a cylindrically shaped electrode. For a negative polarity of the blade electrode, for high and low pressures the lasing was recorded only in the vicinity of this electrode. In the medium pressure domain (200 – 400 Torr), the lasing occupied the greater part of the gap. For a positive polarity of the blade electrode, the output power was substantially lower and the laser beam was recorded only in the vicinity of the blade electrode. The fact that the lasing near the cylindrical electrode does not rise in power with increasing pressure, when the gap is closed by unidirectional ionisation waves, may be attributed to the broadening of the discharge region near this electrode and the propagation of only one ionisation wave. In the case of two blade electrodes, in the counter motion of ionisation waves their leading edges are dominated by oppositely charged particles and, accordingly, a greater enhancement of the electric field is observed.

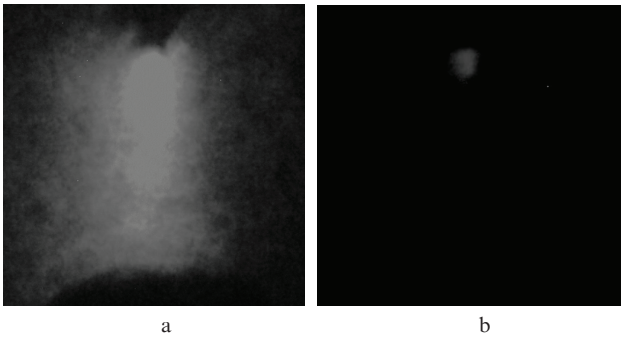

Figure 7. Photographs of the luminescence of white paper under UV irradiation. The nitrogen pressure is $p = 0.3$ atm, the polarity of the blade electrode located above is negative (a) and positive (b) (facility 1).

4. Conclusions

Our investigations show that there occurs UV lasing on the $C\,^3\Pi_u - B^3\Pi_g$ transition for an average value of parameter $E/p < 60$ V cm^{-1} Torr^{-1} in the gap region where diffusive jets (the fronts of ionisation waves) meet at elevated nitrogen pressures. Under these conditions the delay of pulsed lasing from the central gap region was shown to be approximately 1 ns longer than the delay of pulsed lasing from the near-electrode regions. This effect is caused by the enhancement of electric field at the fronts of ionisation waves, the use of two electrodes with a small radius of curvature producing a greater enhancement of the electric field than the use of one electrode with a small radius of curvature. The formation of a diffusive discharge at elevated gas pressures is due to the generation of runaway electrons both near the cathode and in the interspace. The pumping regime which involves the enhancement of electric field between counterpropagating ionisation waves may be employed for obtaining lasing in different

gases. Most appropriate for this regime are transitions with a short lifetime of the upper laser level and a high excitation energy.

Acknowledgements. This work was supported by the Federal Targeted Programme 'Scientific and Scientific-Pedagogic Personnel of Innovative Russia' (State Contract No. 02.740.11.0562).

References

1. Baranov V.Yu., Borisov V.M., Stepanov Yu.Yu. *Electrorazryadnye eksimernye lazery na galogenidakh inertnykh gazov* (Electric-Discharge Excimer Rare-Gas Halide Lasers) (Moscow: Energoatomizdat, 1988).
2. Mesyats G.A., Osipov V.V., Tarasenko V.F. *Pulsed Gas Lasers* (Washington: SPIE Press, 1995).
3. Endo I., Walter R.F. *Gas laser*s (New York: CRC Press, Taylor and Francis Group, 2007).
4. Raizer Yu.P. *Fizika gazovogo razryada* (The Physics of a Gas Discharge) (Dolgoprudnyi: 'Intellekt' Publ. House, 2009).
5. Palmer A.I. *Appl. Phys. Lett*., **25** (3), 138 (1974).
6. Tarasenko V.F., Yakovlenko S.I., Boichenko A.M., et al. *Trudy IOFAN*, **63**, 148 (2007).
7. Raether H.G. *Electron Avalanches and Breakdown in Gases* (London: Butterworths, 1964; Moscow: Energoatomizdat, 1988).
8. Noggle R.C., Krider E.P., Wayland J.R. *J. Appl. Phys*., **39** (10), 4746 (1968).
9. Tarasova L.V., Khudyakova L.N. *Zh. Tekh. Fiz.*, **39** (8), 1530 (1969).
10. Tarasenko V.F., Baksht E.K., Burachenko A.G., Kostyrya I.D., Lomaev M.I., Rybka D.V. *Plasma Devices and Operation*, **16** (4), 267 (2008).
11. Tarasenko V.F. *Fiz. Plazmy*, **37** (5), 444 (2011).
12. Pavlovskii A.I., Buranov S.N., Gorokhov V.V., Karelin V.I., Repin P.B. *Izv. Akad. Nauk SSSR, Ser. Fiz*., **54** (10), 2036 (1990).
13. Buranov S.N., Gorokhov V.V., Karelin V.I., Pavlovskii A.I., Repin P.B. *Kvantovaya Elektron*., **18** (7), 891 (1991) [*Sov. J. Quantum Electron*., **21** (7), 806 (1991)].
14. Derzhiev V.I., Losev V.F., Skakun V.S., Tarasenko V.F., Yakovlenko S.I. *Opt. Spectrosk*., **60** (4), 811 (1986).
15. Alekseev S.B., Gubanov V.P., Kostyrya I.D., Orlovskii V.M., Skakun V.S., Tarasenko V.F. *Kvantovaya Elektron*., **34** (11), 1007 (2004) [*Quantum Electron*., **34** (11), 1007 (2004)].
16. Baksht E.Kh., Burachenko A.G., Tarasenko V.F. *Kvantovaya Elektron.*, **39** (12), 1107 (2009) [*Quantum Electron*., **39** (12), 1107 (2009)].
17. Vasilyak L.M., Kostyuchenko S.V., Kudryavtsev N.N., Filyugin I.V. *Usp. Fiz. Nauk*, **164** (3), 263 (1994).
18. Tarasenko V.F., Tel'minov A.E., Burachenko A.G. *Pis'ma Zh. Tekh. Fiz*., **37** (6), 49 (2011).
19. Tarasenko V.F. *Kvantovaya Elektron*., **31** (6), 489 (2001) [*Quantum Electron*., **31** (6), 489 (2001)].
20. Wagenaars E., Bowden M.D., Kroesen G.M.W. *Phys. Rev. Lett*., **98**, 075002 (2007).